CO_2-Catalyzed One-Electron Oxidations by Peroxynitrite: Properties of the Reactive Intermediate

Sergei V. Lymar[†] and James K. Hurst*

Department of Chemistry, Washington State University, Pullman, Washington 99164-4630

Received July 31, 1997

In neutral bicarbonate-containing solutions, the predominant pathway for peroxynitrite decomposition was CO_2-catalyzed formation of nitrate ion; that is, CO_2 was regenerated in the process. When nitrite ion was present, HCO_3^- also formed during ONO_2^- decomposition. The data could be reproduced by a kinetic model wherein a reactive intermediate formed from ONO_2^- and CO_2 oxidizes NO_2^- to $^\bullet NO_2$, which subsequently hydrolyzes in a bimolecular reaction to form NO_3^- and regenerate NO_2^-. Carbon dioxide catalyzed one-electron oxidations of $Fe(CN)_6^{4-}$, $Mo(CN)_8^{4-}$, $Os(bpy)_3^{2+}$, $Fe(bpy)_3^{2+}$, $Ru(bpy)^{2+}$, and I^- were also observed, establishing that the reactive intermediate is capable of oxidizing compounds whose reduction potentials are as great as 1.3 V. The maximal product yields, measured for reactions with NO_2^-, $Fe(CN)_6^{4-}$, and $Mo(CN)_8^{4-}$, were all ∼35% of the added peroxynitrite, suggesting that they were oxidized by a common intermediate. On the basis of the reactivity characteristics revealed, the intermediate is suggested to be carbonate radical formed by homolytic decomposition of an $ONO_2CO_2^-$ adduct.

Introduction

Peroxynitrite,[1] a strong oxidant,[2] is receiving intensive investigation as a potential pathogenic agent in human disease[3−6] and as a cellularly generated toxin in host defense against invading pathogens.[7−9] This species could be formed by combination of $^\bullet O_2^-$ and $^\bullet NO$ in tissues or cells that simultaneously generate these two radicals[6] or by nitrosation of H_2O_2 by N_2O_3,[10] the latter formed by aerobic oxidation of $^\bullet NO$.[11−13] The protonated form, peroxynitrous acid, oxidizes a wide range of chemical and biochemical compounds, either directly in bimolecular reactions or following rate-limiting unimolecular activation to an intermediate species whose chemical identity is uncertain.[2,14−16] It is also a substrate for peroxidases[17,18] and superoxide dismutase[6] and can both enzymatically[6,18] and nonenzymatically[19] nitrate aromatic groups. The peroxynitrite anion, which is the predominant form above pH 6.8, is a strong nucleophile and forms adducts with metalloporphyrins[20,21] and CO_2.[22−25] The CO_2 adduct may be particularly relevant to the biological reactivity of peroxynitrite because model calculations[26] suggest that, in many physiological fluids,[27] most of the ONO_2^- that might form will be converted to the adduct before reacting with biological targets. In this case, ONO_2^- formation is just the first step in the overall sequence given by

$$^\bullet O_2^- + {}^\bullet NO \rightarrow ONO_2^-$$

$$ONO_2^- + CO_2 \rightarrow ONO_2CO_2^- \qquad (1)$$

Thus, understanding the chemical reactivity of $ONO_2CO_2^-$ is crucial to issues concerning potential biological damage caused by in vivo generation of ONO_2^-.

Carbon dioxide modulates the reactivity of ONO_2^-, altering reaction rates, product yields, and, where multiple products are formed, their distributions. In these reactions, formation of

[†] Current address: Department of Chemistry, Brookhaven National Laboratory, Upton, NY 11973-5000.

(1) Oxoperoxonitrate(1−) (ONO_2^-) and its conjugate acid, hydrogen oxoperoxonitrate (ONO_2H).
(2) Koppenol, W. H.; Moreno, J. J.; Pryor, W. A.; Ischiropoulos, H.; Beckman, J. S. *Chem. Res. Toxicol.* **1992**, *5*, 834.
(3) Rubbo, H.; Darley-Usmar, V.; Freeman, B. A. *Chem. Res. Toxicol.* **1996**, *9*, 809.
(4) Tamir, S.; Burney, S.; Tannenbaum, S. R. *Chem. Res. Toxicol.* **1996**, *9*, 821.
(5) Radi, R. *Chem. Res. Toxicol.* **1996**, *9*, 828.
(6) Beckman, J. S. *Chem. Res. Toxicol.* **1996**, *9*, 836.
(7) Hurst, J. K.; Lymar, S. V. *Chem. Res. Toxicol.* **1997**, *10*, 802.
(8) DeGroote, M. A.; Fang, F. C. *Clin. Infect. Dis.* **1995**, *21*, S162.
(9) Evans, T. J.; Buttery, L. D. K.; Carpenter, A.; Springall, D. R.; Polak, J. M.; Cohen, J. *Proc. Natl. Acad. Sci. U.S.A.* **1996**, *93*, 9553.
(10) Goldstein, S.; Czapski, G. *Inorg. Chem.* **1996**, *35*, 5935.
(11) Ignarro, L. J.; Fukuto, J. M.; Griscavage, J. M.; Rogers, N. E.; Byrns, R. E. *Proc. Natl. Acad. Sci. U.S.A.* **1993**, *90*, 8103.
(12) Lewis, R. S.; Tamir, S.; Tannenbaum, S. R.; Deen, W. M. *J. Biol. Chem.* **1995**, *270*, 29350.
(13) Caulfield, J. L.; Singh, S. P.; Wishnok, J. S.; Deen, W. M.; Tannenbaum, S. R. *J. Biol. Chem.* **1996**, *271*, 25859.
(14) Pryor, W. A.; Squadrito, G. L. *Am. J. Physiol.* **1995**, *268*, L699.
(15) Goldstein, S.; Czapski, G. *Inorg. Chem.* **1995**, *34*, 4041.
(16) Houk, K. N.; Condroski, D. R.; Pryor, W. A. *J. Am. Chem. Soc.* **1996**, *118*, 13002.
(17) Floris, R.; Piersma, S. R.; Yang, G.; Jones. P.; Wever, R. *Eur. J. Biochem.* **1993**, *215*, 767.
(18) Sampson, J. B.; Rosen, H.; Beckman, J. S. *Methods Enzymol.* **1996**, *269*, 210.
(19) van der Vliet, A.; O'Neill, C. A.; Halliwell, B.; Cross, C. E.; Kaur, H. *FEBS Lett.* **1994**, *339*, 89.
(20) Groves, J. T; Marla, S. S. *J. Am. Chem. Soc.* **1995**, *117*, 9578.
(21) Stern, M. K.; Jensen, M. P.; Kramer, K. *J. Am. Chem. Soc.* **1996**, *118*, 8735.
(22) Lymar, S. V.; Hurst, J. K. *J. Am. Chem. Soc.* **1995**, *117*, 8867.
(23) Uppu, R. M.; Squadrito, G. L.; Pryor, W. A. *Arch. Biochem. Biophys.* **1996**, *327*, 335.
(24) Gow, A.; Duran, D.; Thom, S. R.; Ischiropoulos, H. *Arch. Biochem. Biophys.* **1996**, *333*, 42.
(25) Denicola, A.; Freeman, B. A.; Trujillo, M.; Radi, R. *Arch. Biochem. Biophys.* **1996**, *333*, 49.
(26) Lymar, S. V.; Hurst, J. K. *Chem. Res. Toxicol.* **1996**, *9*, 845.
(27) On the basis of relative rate comparisons,[17,26] enzymatic reduction is expected to be the predominant pathway of peroxynitrite disappearance in high peroxidase environments such as the neutrophil phagosome.

S0020-1669(97)00946-4 CCC: $15.00 © 1998 American Chemical Society
Published on Web 01/08/1998

$ONO_2CO_2^-$ (reaction 1) is rate-limiting. Consequently, steady-state concentration levels of $ONO_2CO_2^-$ remain below detectable levels, precluding its direct characterization. As such, its composition is defined only by the rate law. To complicate matters, results from our quantitative mechanistic study[28] on tyrosine nitration by $ONO_2CO_2^-$ indicate that, like peroxynitrous acid,[2,14−16] the CO_2 adduct exists in at least two forms, which exhibit profoundly different chemical reactivities. In this study, we have examined in greater detail the reactions of ONO_2^- with one-electron donors in CO_2-containing media. Collectively, these studies considerably clarify the chemical nature of the reactive intermediate.

Experimental Section

Materials. Potassium octacyanomolybdate(IV)[29] was recrystallized three times from aqueous ethanol. Tris(2,2′-bipyridine)osmium(II) hexafluorophosphate was a gift from Estelle Lebeau and Thomas Meyer (University of North Carolina, Chapel Hill); stock solutions of the more soluble chloride salt were obtained by anion-exchange chromatography on Bio-Rad AG1-X8. Tris(2,2′-bipyridine)iron(II) perchlorate was a gift from John Coddington and Scott Wherland (Washington State University). 2-Ethoxyethyl nitrite was prepared[30] by Qing Tang (Washington State University) and stored over 4-Å molecular sieves at −20 °C. Stock peroxynitrite solutions were prepared by nitrosation of hydroperoxide ion by 2-ethoxyethyl nitrite as follows: 0.1 mL (96 mg) of the organic nitrite was added at room temperature to 24.7 mL of a vigorously stirred 0.3 M sodium hydroxide solution containing a stoichiometric amount of H_2O_2, and the subsequent conversion to sodium peroxynitrite was monitored spectrophotometrically at 302 nm [$\epsilon_{302}(ONO_2^-) = 1.67 \times 10^3\ M^{-1}\ cm^{-1}$].[31] After ∼16 min, the ONO_2^- concentration had reached its maximum (∼33 mM), which corresponded to ∼67% conversion of the 2-ethoxyethyl nitrite. The solution was then frozen and stored at −80 °C. Hydrogen peroxide solutions used in these preparations were standardized by titration with permanganate. The peroxynitrite stock solutons contained as impurities 1 equiv of 2-ethoxyethanol and small amounts of NO_2^-, NO_3^-, and unreacted H_2O_2. The advantages of this preparative method over the commonly used quench-flow reaction[32] between H_2O_2 and NO_2^- is that, unless reaction conditions are carefully controlled,[33] the latter method generates considerably greater amounts of NO_2^- and NO_3^- contaminants. Other chemicals were of the best available grade from commercial suppliers and were used as received. Water was purified using a Milli-Q system.

Analytical Procedures. Optical spectra were measured using a HP 8452 diode array spectrophotometer. Nitrite ion concentrations were determined spectrophotometrically following reaction with sulfanilamide and *N*-(1-naphthyl)ethylenediamine dihydrochloride (Griess reagent).[34] Nitrate ion was determined spectrophotometrically by measuring *Aspergillus* nitrate reductase catalyzed NADPH reduction.[35] Solutions of the enzyme in 50 mM MOPS, pH 7.2, containing 20% glycerol were prepared daily from lyophilized powder (Sigma). Each assay for nitrate content was compared to assays made simultaneously using reference standards whose concentrations bracketed the concentrations of the samples; conversion to nitrite ion was 98−100%.

Chemical Reactions. To analyze for NO_2^- and NO_3^- formed by ONO_2H and $ONO_2CO_2^-$ decompositions, solutions containing known amounts of peroxynitrite ion in 1 mM NaOH were slowly added to rapidly stirred buffer; either the buffer was carbonate-free or 25 mM sodium bicarbonate had been added to it. Conditions were adjusted so that peroxynitrite decay was complete within 10 s after mixing.[22] To determine oxidation−reduction product yields, reactions between ONO_2^- and oxidizable compounds were initiated by flow-mixing equal volumes of solutions using a manually driven two-syringe assembly connected to a 12-jet tangential mixer. One syringe contained the reductant and varying amounts of sodium bicarbonate in phosphate buffer; the pH was adjusted to give the desired initial reactant concentration of CO_2 in the mixed solutions.[36] The other syringe contained ONO_2^- and varying amounts of sodium hydroxide, the concentration of which was adjusted to give the desired final reaction pH in the mixed solutions. Because $ONO_2CO_2^-$ adduct formation[22] (reaction 1) and its subsequent reactions with reductants were much faster than $CO_2-HCO_3^-$ equilibration,[37] the initial concentration of CO_2 following mixing was one-half its concentration in the reactant syringe, and the reaction dynamics were only marginally affected by $CO_2-HCO_3^-$ re-equilibration following the pH jump accompanying mixing. Peroxynitrite concentrations within the reactant syringe were measured within 10 s before mixing by transferring a portion of the solution to an optical cuvette and determining its absorbance at 302 nm. Oxidations of $Fe(CN)_6^{4-}$ and $Mo(CN)_8^{4-}$ were measured from absorption bands due to $Fe(CN)_6^{3-}$ and $Mo(CN)_8^{3-}$ appearing at 420 nm ($\Delta\epsilon_{420} = 1.0 \times 10^3\ M^{-1}\ cm^{-1}$)[38] and 388 nm ($\Delta\epsilon_{388} = 1.2 \times 10^3\ M^{-1}\ cm^{-1}$),[39] respectively; oxidation yields are reported as the ratios of amounts of oxidized product to added peroxynitrite. Oxidations of $Os(bpy)_3^{2+}$, $Fe(bpy)_3^{2+}$, and $Ru(bpy)_3^{2+}$ were monitored from the bleaching of their absorption bands at 650, 500, and 454 nm, respectively; oxidation of I^- was monitored by the formation of I_3^-, which exhibited a strong absorption band at 352 nm. Unless indicated otherwise, these reactions were studied at ambient temperature (23 ± 1 °C).

Stopped-flow kinetics were recorded using a thermostated Hi-Tech SF-40 instrument attached to a Nicolet model 4094B/4562 digital oscilloscope. Kinetic modeling calculations were performed as described in the text using a Mathcad 4.0 computer program. As in the product yield studies, bicarbonate in sufficient concentration to give the desired amount of CO_2 was added to the drive syringe containing the reductant. Experiments to kinetically determine the carbon-containing product of $ONO_2CO_2^-$ decomposition required addition of accurately known small amounts of CO_2 to one of the reactant solutions. This was accomplished by directly injecting metered amounts of bicarbonate from a microsyringe through the tip of a drive syringe that was filled with acidic buffer and had its plunger in place, then mixing with the aid of an entrapped magnetic stirrer bar.

Results and Discussion

Pathways of $ONO_2CO_2^-$ Decomposition. A. Reaction Products. Although it has been widely accepted that proton-catalyzed isomerization to NO_3^- is the only pathway for ONO_2^- decay[40] in neutral to weakly acidic solutions, a recent reinvestigation has revealed a second pathway whose overall stoichiometry is $2ONO_2^- \rightarrow 2NO_2^- + O_2$; the relative contribution of this alternative pathway increased with increasing temperature and medium pH.[41] Under our experimental conditions, the O_2 yield, measured with an O_2-sensing polarographic electrode, was 4−5% of the initial peroxynitrite concentration, indicating only a minor contribution from this alternative pathway.[42] These results are consistent with the published studies, which were made using peroxynitrite prepared by other methods.[41]

Remarkably, we found that no O_2 was produced by peroxynitrite decomposition in bicarbonate-containing solutions.[42] The nitrosoperoxycarbonate adduct could, in principle, decompose

(28) Lymar, S. V.; Jiang, Q.; Hurst, J. K. *Biochemistry* **1996**, *35*, 7855.
(29) Willard, H. H.; Thielke, R. C. *J. Am. Chem. Soc.* **1935**, *57*, 2609.
(30) Noyes, W. A. *J. Am. Chem. Soc.* **1933**, *55*, 3888.
(31) Hughes, M. N.; Nicklin, H. G. *J. Chem. Soc. A* **1968**, 450.
(32) Beckman, J. S.; Chen, J.; Ischiropoulos, H., Crow, J. P. *Methods Enzymol.* **1994**, *233*, 229.
(33) Saha, A.; Goldstein, S.; Cabelli, D.; Czapski, G. *Free Radical Biol. Med.* **1997**, in press.
(34) Greenberg, A. E., Conners, J. J., Jenkins, D., Eds. *Standard Methods for the Examination of Water and Wastewater*, 15th ed, American Public Health Publications: Washington, DC, 1981.
(35) Bories, P. N.; Bories, C. *Clin. Chem.* **1995**, *41*, 904.
(36) Harned, H. C.; Bonner, F. C. *J. Am. Chem. Soc.* **1945**, *67*, 1026.
(37) Kern, D. M. *J. Chem. Educ.* **1960**, *37*, 14.
(38) Jorgensen, C. K. *Acta Chem. Scand.* **1956**, *10*, 518.
(39) Perumareddi, J. R.; Liehr, A. D.; Adamson, A. W. *J. Am. Chem. Soc.* **1963**, *85*, 249.
(40) Edwards, J. O.; Plumb, R. C. *Prog. Inorg. Chem.* **1994**, *41*, 599.
(41) Pfeiffer, S.; Gorren, A. C. F.; Schmidt, K.; Werner, E. R.; Hansert, B.; Bohle, D. S.; Mayer, B. *J. Biol. Chem.* **1997**, *272*, 3465.
(42) Shaw, B. Unpublished observations

by any of several pathways. Hydrolysis would yield bicarbonate and nitrate ions, that is,

$$ONO_2CO_2^- + H_2O \rightarrow NO_3^- + HCO_3^- + H^+ \qquad (2)$$

Heterolytic cleavage of the O−O bond, forming CO_3^{2-} and NO_2^+ as intermediates, would give the same overall reaction since both protonation of carbonate (reaction 9) and hydration of nitronium ion[43] are rapid. Homolytic cleavage of the O−O bond, which calculations suggest is exceptionally weak,[16] would give initially $^{\bullet}NO_2$ and $^{\bullet}CO_3^-$ radicals, that is,

$$ONO_2CO_2^- \rightarrow {}^{\bullet}NO_2 + {}^{\bullet}CO_3^- \qquad (3)$$

which might recombine in various ways to give different products. Radical recombination, which proceeds via O^- transfer to regenerate CO_2,[44] that is,

$$^{\bullet}NO_2 + {}^{\bullet}CO_3^- \rightarrow NO_3^- + CO_2 \qquad (4)$$

would compete with $^{\bullet}NO_2$ dimerization and hydrolysis, the overall reaction being

$$2{}^{\bullet}NO_2 + H_2O \rightarrow NO_2^- + NO_3^- + 2H^+ \qquad (5)$$

In this case, the carbonate radical would also decompose by alternative pathways, most likely via O^- transfer,[44] forming carbon dioxide and peroxycarbonate as immediate products, that is,

$$2{}^{\bullet}CO_3^- \rightarrow CO_2 + CO_4^{2-} \qquad (6)$$

However, the measured rate constant for reaction 4 ($k_4 = 1 \times 10^9$ M^{-1} s^{-1})[44] is 50−100-fold greater than for either reaction 5 [$k_5 = (1.5-6.5) \times 10^7$ M^{-1} s^{-1}][45] or reaction 6 [$k_6 = (0.5-2) \times 10^7$ M^{-1} s^{-1}].[46] Because homolytic cleavage of the O−O bond would yield equal concentrations of $^{\bullet}NO_2$ and $^{\bullet}CO_3^-$, reaction 4 is expected to predominate to the extent that the sole detectable products from decomposition by this pathway will be NO_3^- and CO_2. Finally, intramolecular isomerization accompanied by heterolytic cleavage of the O−C bond would also directly yield NO_3^- and CO_2, that is,

$$ONO_2CO_2^- \rightarrow [O_2NOCO_2^-] \rightarrow NO_3^- + CO_2 \qquad (7)$$

Note that this analysis predicts that, regardless of pathway (reaction 2, 3 plus 4, or 7), the sole nitrogen-containing product will be NO_3^-, although reaction 2 can be distinguished from the others by identification of the carbon-containing product (HCO_3^- versus CO_2).

The product yield in our peroxynitrite preparation was ∼67% (Experimental Section); competing side reactions are hydrolysis of 2-ethoxyethyl nitrite to form NO_2^- during the preparative reaction and ONO_2^- decomposition[41] to form NO_2^- and NO_3^- during synthesis, storage, and handling of the reagent. The extent of contamination of the peroxynitrite reagent was determined by analyzing for NO_2^- and NO_3^- following decomposition of a measured amount of ONO_2^- in carbonate-free buffers. On the basis of measured O_2 yields of ∼4%,[41,42] we assume that ∼8% of the ONO_2^- reacted to produce NO_2^-, with the remaining 92% forming NO_3^-. The differences between measured $[NO_2^-]/[ONO_2^-]_0$ and $[NO_3^-]/[ONO_2^-]_0$ ratios and those expected from the reaction stoichiometry, that is, 0.08 and 0.92, give the amounts of NO_2^- and NO_3^- in the reagent solutions. From the data in Table 1, one calculates that $[NO_2^-]$ and $[NO_3^-]$ were ∼44% and ∼11%, respectively, of the peroxynitrite concentration. Analyses for NO_2^- and NO_3^- after decomposition of ONO_2^- in bicarbonate-containing buffers are also given in Table 1; the concentration of CO_2 was sufficiently high that >99% of the added ONO_2^- decayed through intermediary formation of $ONO_2CO_2^-$ (reaction 1). In this case, the fractional yields corrected for the NO_2^- and NO_3^- originally present in the reagent solution (0.44 and 0.11, respectively) were 0.02 for NO_2^- and 0.99 for NO_3^-. These yields were not influenced by the presence of O_2 or by deliberate addition of H_2O_2. Thus, under all conditions, within experimental uncertainty all of the $ONO_2CO_2^-$ decomposed to give NO_3^-.

Table 1. NO_2^-/NO_3^- Analyses of Decomposed Peroxynitrite Solutions[a]

run no.	$[ONO_2^-]_0$ (μM)	$[NO_2^-]/[ONO_2^-]_0$	$[NO_3^-]/[ONO_2^-]_0$
	Without Added Carbonate[b]		
1	195	0.47	1.09
2	196	0.47	1.08
3	199	0.57	1.01
4	204	0.56	0.94
	av:	0.52 (0.08)	1.03 (0.92)
	With 25 mM Carbonate[c]		
5	193	0.46	1.11
6	198	0.43	1.20
7	205	0.41	1.09
8[d]	195	0.50	1.11
9[e]	183	0.44	1.10
10[f]	197	0.49	0.99
	av:	0.46 (0.02)	1.10 (0.99)

[a] In 25 mM phosphate; each entry is the average of 3 analyses for NO_2^- or 2−3 analyses for NO_3^- from the same product solution; the scatter of individual analyses is ∼5% for NO_2^- and ∼10% for NO_3^-. Numbers in parentheses are the yields of NO_2^- and NO_3^- that are produced from ONO_2^- decomposition (see text). [b] pH 6.5−7.4. [c] pH 7.5−8.0. [d] Anaerobic solution. [e] O_2-saturated solution. [f] 0.6 mM added H_2O_2.

The carbon-containing reaction product can be identified from kinetic decay profiles under conditions where the CO_2 concentration is much lower than ONO_2^-. Specifically, if HCO_3^- is the product, CO_2 will be depleted from the medium and the overall reaction will quickly become rate-limited by its reformation by dehydration of HCO_3^-. This follows because, under the experimental conditions (pH 8), both HCO_3^-−CO_2 equilibration ($t_{1/2} \simeq 25$ s) and uncatalyzed decomposition of ONO_2^- ($t_{1/2} \simeq 9$ s) are considerably slower than the reaction between ONO_2^- and CO_2 ($t_{1/2} \simeq 0.9$ s). Consequently, the kinetics of ONO_2^- disappearance will be markedly biphasic, with the breakpoint occurring at a concentration of decomposed peroxynitrite that is approximately equal to the initial concentration of CO_2. In contrast, if CO_2 is the product, its concentration will not change over the time course of the reaction, and simple first-order kinetic behavior will be observed.

When these reactions were carried out, ONO_2^- decay was found to be nearly first order, even when the peroxynitrite concentration was in large excess. This behavior is illustrated in Figure 1a (lower trace and inset), where the initial peroxynitrite concentration is 5-fold greater than the CO_2 concentration.

(43) Moodie, R. B.; Schofield, K.; Taylor, P. G. *J. Chem. Soc., Perkin Trans. 2* **1979**, 133.
(44) Lilie, J.; Hanrahan, R. J., Henglein, A. *Radiat. Phys. Chem.* **1978**, *11*, 225.
(45) Neta, P.; Huie, R. E.; Ross, A. B. *J. Phys. Chem. Ref. Data* **1988**, *17*, 1027.
(46) Pryor, W. A., Lemercier, J.-N.; Zhang, H.; Uppu, R. M.; Squadrito, G. L. *Free Radical Biol. Med.* **1997**, *23*, 331.

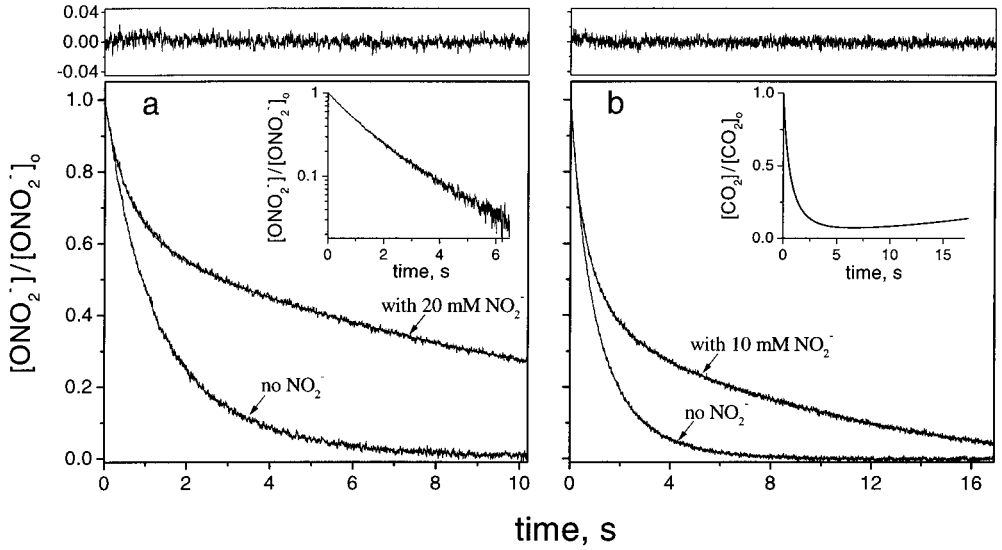

Figure 1. Stopped-flow kinetics of peroxynitrite decay with $[ONO_2^-]_0 > [CO_2]_0$. (a) Lower trace: 56 μM CO_2 in 0.2 M phosphate, pH 4.34, mixed with an equal volume of 280 μM ONO_2^- in 0.19 M NaOH (final pH 7.90); the inset gives a semilogarithmic presentation of this curve. Upper trace: reaction under identical medium conditions except 20 mM NO_2^- present in the final solution and $[ONO_2^-] = 456$ μM before mixing. (b) Lower trace: 76 μM CO_2 (5.5 mM total carbonate) in 0.21 M phosphate, pH 7.95 mixed with an equal volume of 460 μM ONO_2^- in 6 mM NaOH (final pH 8.36). Upper trace: reaction under identical medium conditions except 10 mM NO_2^- present in the final solution and $[ONO_2^-] =$ 436 μM before mixing; the inset shows the temporal behavior of the CO_2 concentration for this experiment calculated from kinetic modeling. All reactions were at 24 °C. Upper panels are the residuals from kinetic data fits for the NO_2^--containing solutions according to eqs 10 and 11 as described in the text using $k_1 = 3 \times 10^4$ M^{-1} s^{-1} and the following other parameters: panel a, $k_0 = 0.080$ s^{-1}, $A = 0.33$; panel b, $k_0 = 0.037$ s^{-1}, $[CO_2]_{eq} = 15$ μM, $R = 1.1$ μM/s, $A = 0.25$.

To ensure that the result was not somehow dependent upon the pH jump, analogous experiments were performed in which the pH change upon mixing was small; equivalent results were obtained (Figure 1b, lower trace). Since complete decomposition in this case requires on average five cycles of each CO_2 molecule, it is evident that CO_2 is the species regenerated on each cycle and is acting as a true catalyst. These observations confirm results of a recent study by Pryor and co-workers, who have also concluded that CO_2 is the carbon-containing product of $ONO_2CO_2^-$ decomposition.[46] The small deviations from exponential behavior observed at the later stages of reaction (Figure 1a, inset) can, at least in part, be attributed to a small decrease in CO_2 concentration arising from (i) hydration to HCO_3^- and (ii) reaction with NO_2^- (described below), which was present as a contaminant of the peroxynitrite reagent at a concentration of 65−110 μM in the final reaction solutions. The results indicate that mechanisms yielding bicarbonate as a product, that is, those involving hydrolysis of $ONO_2CO_2^-$ (reaction 2) or heterolytic cleavage of the O−O bond to form NO_2^+ and CO_3^{2-}, do not contribute appreciably to $ONO_2CO_2^-$ decomposition.

B. Influence of Nitrite Ion. In agreement with earlier reports,[31] we detected no influence of nitrite ion upon the rates of ONO_2^- decay in carbonate-free buffers. However, in the presence of CO_2, where decomposition proceeds through the intermediacy of $ONO_2CO_2^-$, addition of NO_2^- dramatically changed the decay kinetics (Figure 1a,b, upper traces). In these cases, the initial rates were nearly the same as for solutions without added nitrite, but the decay rapidly decelerated over the course of the reaction. This behavior indicates that CO_2 was being taken out of the catalytic cycle represented by reactions 1, 3, and 4 (or 1 and 7). We have demonstrated elsewhere[22,28] and will present additional evidence hereinafter that $ONO_2CO_2^-$ is a strong one-electron oxidant. It is therefore reasonable to postulate that the effect of nitrite is due to its one-electron oxidation, yielding

$$ONO_2CO_2^- + NO_2^- \rightarrow 2^{\bullet}NO_2 + CO_3^{2-} \quad (8)$$

followed by fast carbonate protonation, that is,

$$CO_3^{2-} + H^+ \rightarrow HCO_3^- \quad (9)$$

and $^{\bullet}NO_2$ radical combination and hydrolysis (reaction 5). Summation of reactions 5, 8, and 9 generates reaction 2. An alternative but equivalent mechanism involving direct formation of dinitrogen tetroxide, that is, $ONO_2CO_2^- + NO_2^- \rightarrow N_2O_4 + CO_3^{2-}$, is possible, but seems less likely because it involves extensive molecular rearrangement. In any event, the final result of reaction 8 is the same as $ONO_2CO_2^-$ hydrolysis in which HCO_3^- is formed, temporarily removing CO_2 from the catalytic cycle. On longer time scales, however, dehydration of HCO_3^- will regenerate CO_2 to its equilibrium level. Nitrite is also regenerated in reaction 5. Thus, reactions 1, 5, 8, and 9 involve two coupled catalytic processes, that is, CO_2-catalyzed peroxynitrite isomerization and NO_2^--catalyzed CO_2 hydration.

The proposed mechanism can be evaluated quantitatively. The lifetime of the $ONO_2CO_2^-$ adduct is sufficiently short ($t_{1/2} \leq 1$ ms)[28] that it does not accumulate during reaction. By applying the steady-state approximation to $ONO_2CO_2^-$ and treating the concentration of NO_2^- (present in large excess) as a constant, the following rate laws are derived:

$$-d[ONO_2^-]/dt = (k_0 + k_1[CO_2])[ONO_2^-] \quad (10)$$

$$-d[CO_2]/dt = Ak_1[CO_2][ONO_2^-] \quad (11)$$

In these equations, k_0 is the apparent rate constant[47] for ONO_2^- decay in the absence of CO_2, which was determined in separate experiments under identical medium conditions, and $k_1 = 3 \times 10^4$ M^{-1} s^{-1} is the previously determined[22] rate constant for reaction 1. The factor A introduced in eq 11 represents the

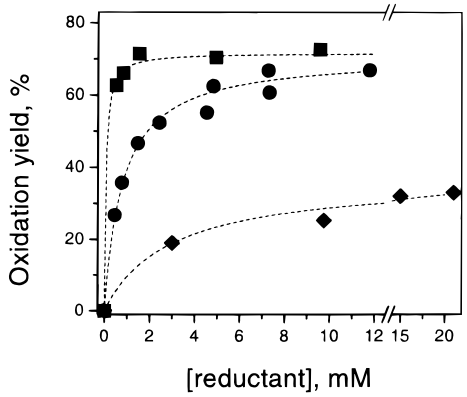

Figure 2. Product yields for CO_2-catalyzed one-electron oxidations by peroxynitrite measured for $Fe(CN)_6^{4-}$ (squares) and $Mo(CN)_8^{4-}$ (circles) and calculated as described in the text for NO_2^- (diamonds). Note abscissa break at 12 mM reductant concentrations. Reaction conditions for cyanide complexes: 0.1 M phosphate, pH 7.1−7.2, 19 mM total carbonate, concentration of ONO_2^- was varied within 190−400 μM range. For lower curve reaction conditions see Figure 1 and the text.

fraction of $ONO_2CO_2^-$ that participates in oxidation of NO_2^-, thereby generating HCO_3^- (reaction 8). In these rate laws, the relatively slow $CO_2-HCO_3^-$ hydration−dehydration equilibration has been ignored. The reactions with NO_2^- present were modeled by simultaneously numerically integrating eqs 10 and 11 for different values of A until the best fit was found. As is apparent from the residuals of the fit to the experimental data (Figure 1a), the kinetic model accurately reproduces the observed reaction dynamics.

When the medium contained higher concentrations of bicarbonate ion (Figure 1b), $CO_2-HCO_3^-$ equilibration could no longer be ignored in the kinetic modeling. Including this reaction did not change eq 10, but added a second term to eq 11, that is,

$$-\mathrm{d}[CO_2]/\mathrm{d}t = Ak_1[CO_2][ONO_2^-] - R(1 - [CO_2]/[CO_2]_{eq})$$

where R is the rate of HCO_3^- dehydration and $[CO_2]_{eq}$ is the concentration of CO_2 at equilibrium. Under the experimental conditions, R was practically constant (with a calculated value[48] of 1.1 μM/s) because HCO_3^- was in large excess over $[CO_2]_{eq}$ (15 μM).[36] Using these values as constants, with A as the only variable parameter, it was again possible to obtain a near-perfect fit to the experimental data (Figure 1b, residual plot). The influence of $CO_2-HCO_3^-$ equilibration is evident in the calculated plot of the variation in CO_2 concentration with time (Figure 1b, inset). Specifically, HCO_3^- dehydration prevented complete depletion of CO_2 from the medium and allowed partial recovery toward equilibrium values in the later stages of the reaction. Nonetheless, omitting this reaction from the analysis by setting $R = 0$ had little effect on the fit to the experimental curves and reduced the calculated best-fit value of A by only about 10%.

The values of A determined for a series of experiments in which the nitrite concentration was varied are given in Figure 2. Interference from UV absorption by NO_2^- made it impractical to use concentrations higher than 20 mM. The curve saturated at $A \simeq 0.35$, suggesting that maximally only 35% of the $ONO_2CO_2^-$ is capable of oxidizing the NO_2^- ion.

In previous publications, we had reported observation of biphasic kinetics similar to the upper traces in Figure 1a,b under conditions where the total peroxynitrite concentration exceeded the CO_2 concentration, but in which NO_2^- was not deliberately added to the medium.[22,49] These were provisionally interpreted as indicating $ONO_2CO_2^-$ decomposition by hydrolysis, that is, reaction 2. In those studies, we prepared peroxynitrite stock solutions by reacting H_2O_2 with NO_2^-, which resulted in relatively high nitrite ion contamination. We now recognize that these effects were due instead to nitrite oxidation, leading to HCO_3^- formation (reactions 8 and 9). Experiments described below will show that the presence of nitrite can also strongly distort CO_2-catalyzed peroxynitrite oxidation reactions.

Oxidation of Inorganic Compounds. A. General Considerations. The three major pathways for ONO_2^- decay are proton-catalyzed isomerization, reaction with CO_2, and direct oxidation of other compounds (when present). Unless otherwise specified, for the experiments described below the CO_2 concentration was maintained in sufficiently high concentration to ensure that the dominant pathway was through formation of the $ONO_2CO_2^-$ adduct (reaction 1). Consequently, the oxidant for all reactions described in this section was $ONO_2CO_2^-$ or a species derived from it.

B. Cyanide Complexes of Fe(II) and Mo(IV). We have confirmed Goldstein and Czapski's observations[15] that peroxynitrite in carbonate-free media oxidizes $Fe(CN)_6^{4-}$ to $Fe(CN)_6^{3-}$ by a pathway that is first-order in ONO_2^- and independent of the $Fe(CN)_6^{4-}$ concentration. Peroxynitrite also oxidized $Mo(CN)_8^{4-}$ to $Mo(CN)_8^{3-}$ in a reaction whose rate was independent of the $Mo(CN)_8^{4-}$ concentration; for this reaction the apparent first-order rate constant for $Mo(CN)_8^{3-}$ formation was identical to the rate constant for peroxynitrite decay in the absence of reductant under otherwise identical conditions (data not shown). The kinetics indicate that neither $Fe(CN)_6^{4-}$ nor $Mo(CN)_8^{4-}$ reacted directly with peroxynitrite, but rather that the rate-limiting step for these reactions is the same unimolecular activation that is required for proton-catalyzed peroxynitrite decomposition.[40]

Rates of one-electron oxidations of the cyanide complexes were greatly accelerated when CO_2 was present in the medium. Rate laws for the oxidations were identical to the rate law for CO_2-catalyzed peroxynitrite decay, indicating that reaction 1 was rate-limiting. Oxidation of the complexes could occur via reactions analogous to reaction 8, that is,

$$ONO_2CO_2^- + M(CN)_n^{4-} \rightarrow {}^{\bullet}NO_2 + CO_3^{2-} + M(CN)_n^{3-} \quad (12)$$

The $^{\bullet}NO_2$ radical generated is a sufficiently strong one-electron oxidant, with $E°(^{\bullet}NO_2/NO_2^-) = 1.04$ V,[50,51] to oxidize both $Fe(CN)_6^{4-}$ ($E° = 0.36$ V)[52] and $Mo(CN)_8^{4-}$ ($E° = 0.73$ V),[52] that is,

$$^{\bullet}NO_2 + M(CN)_n^{4-} \rightarrow NO_2^- + M(CN)_n^{3-} \quad (13)$$

For $Fe(CN)_6^{4-}$, the reported rate constant[53,54] for reaction 13 is

(47) The form of peroxynitrite that undergoes spontaneous isomerization is peroxynitrous acid (HOONO).[40] In alkaline solutions, the predominant form of peroxynitrite is the conjugate base; under these conditions, the rate law can be expressed as $-\mathrm{d}[ONO_2^-]/\mathrm{d}t = k_0[ONO_2^-]$. The pH-dependent rate constant $k_0 = k[H^+]/([H^+] + K_a)$, where k and K_a are the HOONO isomerization rate constant and acid dissociation constant, respectively.

(48) Gibbons, B. H.; Edsall, J. T. *J. Biol. Chem.* **1963**, *238*, 3502.

(49) Hurst, J. K. *Adv. Chem. Ser.***1997**, *253*, 399.

(50) Stanbury, D. M. *Adv. Inorg. Chem.* **1989**, *33*, 69.

(51) All potentials reported are referenced against NHE.

(52) Latimer, W. M. *Oxidation Potentials*, 2nd ed.; Prentice-Hall: New York, 1952.

(53) Ottolenghi, M.; Rabani, J. *J. Phys. Chem.* **1968**, *72*, 593.

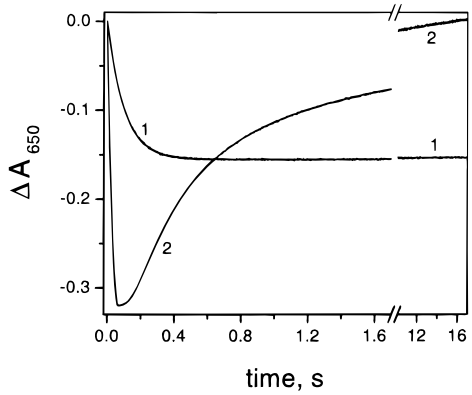

Figure 3. Stopped-flow kinetics of CO_2-catalyzed oxidation of Os(bpy)$_3^{2+}$ by peroxynitrite monitored at 650 nm. Conditions following mixing at 20 °C in 0.12 M phosphate were as follows: trace 1, [Os(bpy)$_3^{2+}$] = 125 μM, [ONO_2^-] = 76 μM, [carbonate] = 5.6 mM, [NO_2^-] ≈ 34 μM, pH 6.1; trace 2, [Os(bpy)$_3^{2+}$] = 100 μM, [ONO_2^-] = 440 μM, [carbonate] = 23 mM, [NO_2^-] = 2.6 mM, pH 5.4. Note abscissa break at 1.7 s.

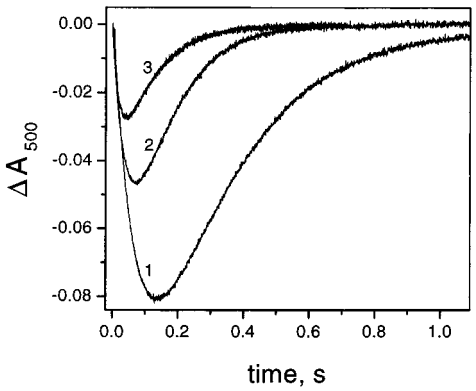

Figure 4. Stopped-flow kinetics of CO_2-catalyzed oxidation of Fe(bpy)$_3^{2+}$ by peroxynitrite monitored at 500 nm. Conditions following mixing at 20 °C in 0.12 M phosphate were as follows: trace 1, [Fe(bpy)$_3^{2+}$] = 42 μM, [ONO_2^-] = 75 μM, [carbonate] = 5.6 mM, [NO_2^-] ≈ 33 μM, pH 6.1; trace 2, [NO_2^-] ≈ 150 μM, other conditions the same; trace 3, [NO_2^-] ≈ 370 μM, other conditions the same.

(3−4.3) × 10^6 M^{-1} s^{-1}. Under our experimental conditions, this reaction is sufficiently rapid that it will completely dominate the competing pathway for $^{\bullet}NO_2$ decay (reaction 5).[55] According to reactions 12 and 13, the maximum stoichiometric yield of oxidized product that could be attained in these reactions is 200% of the added ONO_2^-. A striking feature of these reactions is that both yields reach saturating values at high complex concentrations of 65−70% of the added oxidant (Figure 2). This result implies that, although the reaction proceeds nearly completely via reaction 1, only ∼35% of the $ONO_2CO_2^-$ formed is capable of reacting with the complexes, with the remainder apparently decomposing to NO_3^- and CO_2.

C. Tris(bipyridyl) Complexes of Fe(II), Os(II), and Ru(II). The reactions of these complexes with $ONO_2CO_2^-$ were monitored by measuring the bleaching of their visible absorption bands (Figures 3−5). These reactions were run in slightly acidic solution to minimize interferences arising from

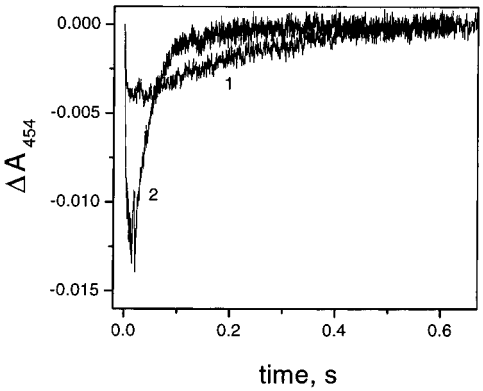

Figure 5. Stopped-flow kinetics of CO_2-catalyzed oxidation of Ru(bpy)$_3^{2+}$ by peroxynitrite monitored at 454 nm. Conditions following mixing at 20 °C in 0.12 M phosphate were as follows: trace 1, [Ru(bpy)$_3^{2+}$] = 34 μM, [ONO_2^-] = 76 μM, [carbonate] = 5.6 mM, [NO_2^-] ≈ 34 μM, pH 6.1; trace 2, [Ru(bpy)$_3^{2+}$] = 25 μM, [ONO_2^-] = 600 μM, [carbonate] = 22 mM, [NO_2^-] ≈ 280 μM, pH 6.2.

reactions of the corresponding trivalent ions with hydroxide ion.[56] Flow-mixing Os(bpy)$_3^{2+}$ with peroxynitrite in buffered carbonate solution led to bleaching of the absorption band at a rate that corresponded to the rate of peroxynitrite decay given by reaction 1 (Figure 3, trace 1). The product was relatively stable, but underwent slow back-conversion to Os(bpy)$_3^{2+}$ over a period of several minutes. Because Os(bpy)$_3^{2+}$ absorbs relatively strongly throughout the visible region and has relatively low solubility, it was not possible to determine the limiting oxidation yields as was done for the cyanide complexes (Figure 2). When millimolar concentrations of NO_2^- were added to the solution, the recovery of Os(bpy)$_3^{2+}$ following bleaching was markedly accelerated (Figure 3, trace 2). The apparent greater extent of Os(bpy)$_3^{2+}$ oxidation in trace 2 is a consequence of the higher concentration of peroxynitrite used for that run. Upon completion of the reaction, the optical spectrum was identical to the initial Os(bpy)$_3^{2+}$ spectrum, indicating that the oxidative bleaching was reversible. When Fe(bpy)$_3^{2+}$ was used as the reductant, the return reaction was rapid even in the absence of added NO_2^- (Figure 4, trace 1). As described previously, these solutions contained ∼33 μM NO_2^-, introduced as a contaminant in the peroxynitrite. Addition of submillimolar amounts of NO_2^- greatly accelerated the return reaction (Figure 4, traces 2 and 3); the net maximal amount of bleaching and the time interval between mixing and reaching the absorbance minimum decreased with increasing NO_2^- concentrations. These features are consistent with the following set of reactions:

$$ONO_2CO_2^- + M(bpy)_3^{2+} \rightarrow {}^{\bullet}NO_2 + CO_3^{2-} + M(bpy)_3^{3+} \quad (14)$$

$$M(bpy)_3^{3+} + NO_2^- \rightleftarrows {}^{\bullet}NO_2 + M(bpy)_3^{2+} \quad (15)$$

On the basis of the standard one-electron reduction potentials[51] for the complexes [$E°$(Os(bpy)$_3^{3+/2+}$) = 0.84 V;[57] $E°$(Fe(bpy)$_3^{3+/2+}$) = 1.05 V;[58] $E°$(Ru(bpy)$_3^{3+/2+}$) = 1.26 V[56]], the calculated equilibrium constants for reaction 15 are 4.0 × 10^{-4}, 1.5, and 5.0 × 10^3, respectively. For Fe(CN)$_6^{3-}$ and Mo(CN)$_8^{3-}$ with NO_2^-, the corresponding values are 3.2 ×

(54) Buxton, G. V. *Trans. Faraday Soc.* **1969**, *65*, 2150.
(55) Under our conditions, [Fe(CN)$_6^{4-}$] ≥ 1 mM, so that $t_{1/2} \leq 0.2$ ms for reaction 13; the rate of $^{\bullet}NO_2$ formation equals the rate of $ONO_2CO_2^-$ decomposition (limited by reaction 1, which is less than 5 × 10^{-3} M/s). Combined with reaction 5, one calculates a *maximal* steady-state concentration for $^{\bullet}NO_2$ that is less than 1 μM. Consequently, $t_{1/2}$ > 10 ms for reaction 5, indicating that it is insignificant in the presence of Fe(CN)$_6^{4-}$.
(56) Creutz, C.; Sutin, N. *Proc. Natl. Acad. Sci. U.S.A.* **1975**, *72*, 2858.
(57) Szentrimay, R.; Yeh, P.; Kuwana, T. *ACS Symp. Ser.* **1977**, *38*, 143.
(58) Sutin, N.; Creutz, C. *Pure Appl. Chem.* **1980**, *52*, 2717.

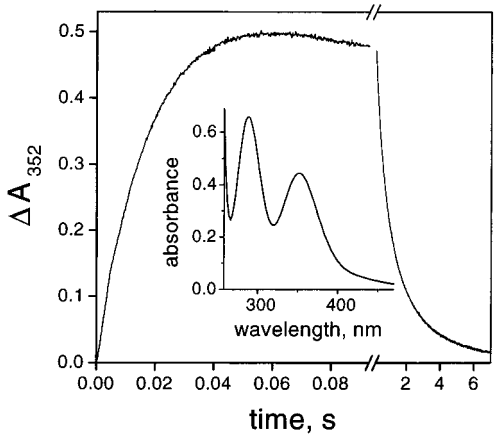

Figure 6. Stopped-flow kinetics of CO_2-catalyzed oxidation of I^- by peroxynitrite: 20 mM KI plus 46.7 mM total carbonate in 0.20 M phosphate, pH 7.2, mixed at 20 °C with 185 μM ONO_2^- in 60 mM NaOH (final pH 9.4); the inset shows the optical spectrum of the transient species taken 100−200 ms following mixing.

10^{-12} and 5.0×10^{-6}, respectively. The relatively slow reduction of $Os(bpy)_3^{3+}$ arises from the unfavorable equilibrium position of reaction 15 which, nonetheless, was driven to completion by the disproportionation of $^{\bullet}NO_2$ (reaction 5). In contrast, reduction of $Fe(bpy)_3^{3+}$ was much faster even at low NO_2^- concentrations because the equilibrium position was displaced to the right. On the basis of these considerations, one anticipates high sensitivity to contaminating nitrite in the oxidation of $Ru(bpy)_3^{2+}$ by $ONO_2CO_2^-$. Indeed, only a very small (but reproducible) bleaching, corresponding to 1−2 μM conversion to $Ru(bpy)_3^{3+}$, was observed from reacting $Ru(bpy)_3^{2+}$ with $ONO_2CO_2^-$. Even if it were possible to prepare nitrite-free peroxynitrite reagents, NO_2^- formed via reactions 14 and 5 would be sufficient to rapidly reduce the oxidized ruthenium complex. The overall apparent result of reversible oxidation of the $M(bpy)_3^{2+}$ ions by $ONO_2CO_2^-$ is reaction 2. Thus, these ions present an additional pathway for redox-mediated hydrolysis of $ONO_2CO_2^-$ to NO_3^- and HCO_3^-.

D. Iodide Ion. Iodide ion has been shown to undergo direct bimolecular reaction with peroxynitrous acid, but no reaction was detected with the peroxynitrite anion.[15] To avoid interference by the direct reaction between I^- and ONO_2H with $ONO_2CO_2^-$ formation, we studied the oxidation of I^- by $ONO_2CO_2^-$ in alkaline solutions. The pH-jump technique was used to generate a large nonequilibrium concentration of CO_2 in the mixed solutions. This procedure ensured that virtually all of the peroxynitrite present formed the $ONO_2CO_2^-$ adduct prior to subsequent reaction with iodide. Stopped-flow experiments indicated fast formation of a transient species that absorbed strongly at 352 nm when solutions containing CO_2 and I^- were mixed with peroxynitrite (Figure 6). The optical spectrum of this species was obtained in a continuous-flow experiment using a manually driven two-syringe mixer directly attached to the diode array spectrophotometer. This spectrum, obtained at 100−200 ms after mixing (Figure 6, inset), corresponds to the published I_3^- spectrum,[59] thus identifying it as the transient species. The characteristic time for I_3^- formation was determined from the stopped-flow kinetic trace to be $t_{1/2} \simeq 11$ ms, which is very nearly identical to the CO_2-catalyzed ONO_2^- decay time ($t_{1/2} \simeq 15$ ms) measured under these conditions in the absence of I^-. On the basis of reported data,[15] the calculated half-time for direct reaction between ONO_2H and I^- under these conditions is $t_{1/2} \simeq 460$ ms. We therefore conclude that the observed reaction (Figure 6) constitutes oxidation of I^- by $ONO_2CO_2^-$.

Under the experimental conditions, I_3^- (rather than HOI) is the stable form of the oxidized iodide.[60] Consequently, formation of I_3^- via intermediary two-electron oxidation of I^- to HOI by $ONO_2CO_2^-$, that is, $ONO_2CO_2^- + I^- + H^+ \rightarrow NO_2^- + CO_2 + HOI$, followed by

$$HOI + H^+ + 2I^- \rightarrow I_3^- + H_2O \qquad (16)$$

cannot be excluded on thermodynamic grounds. However, the rate law for reaction 16 determined in unbuffered solutions is $R = (4.4 \times 10^{12}\ M^{-2}\ s^{-1})[HOI][H^+][I^-]$;[63] from these data, the calculated half-time for reaction 16 under our experimental conditions is $t_{1/2} \simeq 40$ ms, that is, 4-fold slower than the observed rate of I_3^- appearance. Further, the absence of a detectable induction period in the kinetic trace (Figure 6) indicates that, if HOI were a precursor to I_3^- formation, it must decay with $t_{1/2} \leq 1-2$ ms, that is, within the mixing time of the experiment. Thus, either reaction 16 is strongly catalyzed by the medium buffer or HOI is not an intermediate on the pathway for I^- oxidation to I_3^- by $ONO_2CO_2^-$. The latter alternative implies that the reaction is a one-electron oxidation, that is,

$$ONO_2CO_2^- + I^- \rightarrow {}^{\bullet}NO_2 + CO_3^{2-} + {}^{\bullet}I \qquad (17)$$

The iodine atom formed in solutions containing high concentrations of I^- will rapidly generate I_3^- via the following sequence:[45] $^{\bullet}I + I^- \rightarrow {}^{\bullet}I_2^-$ and $2{}^{\bullet}I_2^- \rightarrow I_3^- + I^-$. The slow subsequent loss of I_3^- observed in the kinetic traces (Figure 6) can be attributed to its disproportionation to IO_3^- and I^- via the intermediacy of HOI. This reaction is complex[64] and was not analyzed in this study.

General Conclusions. A. Reaction Mechanisms. The following properties of the $ONO_2CO_2^-$ intermediate can be deduced from our observations: First, in the absence of reductants, $ONO_2CO_2^-$ decomposes nearly quantitatively to NO_3^- and CO_2. Since CO_2 is the carbonate species that reacts with ONO_2^- to form the adduct,[22] it functions as a catalyst for ONO_2^- isomerization to NO_3^-. Similar conclusions have recently been reached by Pryor and co-workers.[46] Second, only a minor fraction (~35%) of the $ONO_2CO_2^-$ formed can engage in one-electron oxidations, indicating the presence of at least two intermediary species, one of which cannot be scavenged even by very easily oxidized ions such as $Fe(CN)_6^{4-}$. Goldstein and Czapski have also reported an oxidation yield of 33% for reaction of $ONO_2CO_2^-$ with $Fe(CN)_6^{4-}$, Ni^{II}(cyclam), and the redox-active dye ABTS (2,2′-azinobis(3-ethyl-1,2-dihydrobenzothiazoline-6-sulfonate).[65] Because the rate-limiting step in these reactions is formation of $ONO_2CO_2^-$, the kinetics of the redox reactions cannot be directly determined. Nonetheless,

(59) Meyerstein, D.; Treinin, A. *Trans. Faraday Soc.* **1963**, *59*, 1114.

(60) From reported constants for the equilibria $I_2 + H_2O \rightleftharpoons HOI + H^+ + I^-$ ($K = 2.0 \times 10^{-13}\ M^2$)[61] and $I_2 + I^- \rightleftharpoons I_3^-$ ($K = 710\ M^{-1}$),[62] one calculates $[HOI]/[I_3^-] = 1.8 \times 10^{-3}$ for the conditions given in Figure 6.

(61) Cotton, F. A.; Wilkinson, G. *Advanced Inorganic Chemistry*, 3rd ed.; Interscience: New York, 1972.

(62) Downs, A. J.; Adams, C. J. In *Comprehensive Inorganic Chemistry*; Bailar, J. C., Jr., Emeleus, H. J., Nyholm, R., Trotman-Dickenson, A. F., Eds.; Pergamon Press: Oxford, 1973; Chapter 26.

(63) Eigen, M.; Kustin, K. *J. Am. Chem. Soc.* **1962**, *84*, 1355.

(64) Urbansky, E. T.; Cooper, B. T.; Margerum, D. W. *Inorg. Chem.* **1997**, *36*, 1338.

(65) Goldstein, S.; Czapski, G. *Inorg. Chem.* **1997**, *36*, 5113.

Scheme 1

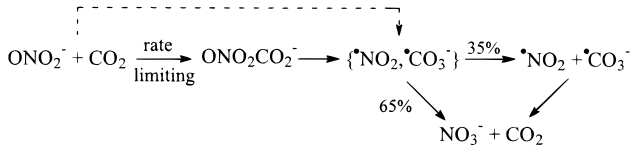

the near constancy of limiting product yields for oxidation of NO_2^-, $Fe(CN)_6^{4-}$, Ni^{II}(cyclam), ABTS, and $Mo(CN)_8^{4-}$ suggests that these reactions involve a common oxidizing intermediate. Third, the reactive form of $ONO_2CO_2^-$ is a very strong oxidant that is capable of oxidizing even $Fe(bpy)_3^{2+}$, $Ru(bpy)_3^{2+}$, and I^-, whose reduction potentials are 1−1.3 V.

The existence of two different intermediates, one reactive and the other unreactive, has also been demonstrated for reactions involving ONO_2H as oxidant. It has further been suggested that the two forms are cis and trans conformational isomers.[2,14,15] However, for $ONO_2CO_2^-$, it is difficult to imagine how changes in molecular conformation could lead to differences in oxidizing potential between reactive and unreactive intermediates as large as has been observed. A more plausible explanation is that the unreactive intermediate is too short-lived to engage in bimolecular reactions. Although these studies do not establish the identities of these species, one notes that the chemical properties of the reactive form of $ONO_2CO_2^-$ are consistent with those of carbonate radical ($•CO_3^-$), for which $E°(•CO_3^-/CO_3^{2-}) = 1.5$ V.[50] A mechanism for $ONO_2CO_2^-$ decomposition through formation of $•CO_3^-$ is presented in Scheme 1, wherein $\{•NO_2,•CO_3^-\}$ represents a geminate radical pair produced by homolytic cleavage of the O−O bond in the adduct. (The geminate radical pair could, in principle, be formed directly by O^- transfer from ONO_2^- to CO_2; this pathway is shown by a dashed arrow.) Because only radicals escaping the solvent cage can react with solutes, the limiting oxidation yield of 35% represents the cage escape yield. Consistent with this mechanism, O^- transfer[44] from $•CO_3^-$ to $•NO_2$, both in the geminate pair and in solvent-separated species, leads directly to formation of CO_2 and NO_3^-, as observed. Within this scenario, the actual oxidant in reactions 8, 12, 14, and 17 is the $•CO_3^-$ radical. The second product of $ONO_2CO_2^-$ decomposition, that is, $•NO_2$, readily oxidized $Fe(CN)_6^{4-}$ and $Mo(CN)_8^{4-}$, but reaction with NO_2^- is simply electron exchange, accounting for the 2-fold greater saturating yield in the former reactions (Figure 2). Formation of $•CO_3^-$ during peroxynitrite decay in alkaline carbonate buffers has also been suggested from chemiluminescence measurements.[25]

A recent estimation places the free energy of formation of ONO_2H at 7.7 kcal/mol,[66] which is ∼7 kcal/mol higher than earlier estimates.[2] Using this most recent value together with known free energies of formation for CO_2, $•NO_2$, and $•CO_3^-$,[50] we calculate that the thermodynamic driving force for reaction, $ONO_2^- + CO_2 \rightarrow •NO_2 + •CO_3^-$, is $\Delta G° = -1.4$ kcal/mol. These calculations suggest, therefore, that the proposed free-radical mechanism is plausible on thermodynamic grounds.

B. Biological Implications. Evidence is accumulating to suggest that peroxynitrite plays an important role in the pathogenesis of human disease associated with oxidative stress.[3−9] The present studies establish that $ONO_2CO_2^-$ produces a powerful oxidant, suggested to be $•CO_3^-$ radical, that is capable of inflicting extensive damage on biomolecules. The $•CO_3^-$ radical, for example, is capable of selective oxidation of several critical amino acids in proteins[67,68] and is bactericidal;[69] model calculations suggest that, when confined to subcellular compartments, a major fraction of the $•CO_3^-$ generated could survive scavenging by antioxidants present in biological fluids to react with cellular target sites.[70] Potential roles for NO_2^- and $•NO_2$ are also suggested by these studies. Nitrite ion is found in normal biological fluids at concentrations as high as 200 μM and can reach substantially higher levels under pathogenic conditions;[71] its accumulation can be ascribed to $•NO$ generation by nitric oxide synthases, followed by a reaction sequence involving aerobic oxidation to $•NO_2$, combination with excess $•NO$ to form N_2O_3, and its hydration to NO_2^-.[11−13] A potential additional pathway for NO_2^- formation is from $ONO_2CO_2^-$ in reactions with biological reductants analogous to those described for the $M(CN)_x^{4-}$ ions (reaction 12), although physiological concentration levels of NO_2^- are not likely to be sufficiently high for substantive participation of reaction 8 in biological processes (Figure 2). Possible protection of cellular tissues from strong oxidants by biologically derived NO_2^- is also suggested by the relatively rapid reduction of $M(bpy)_3^{3+}$ ions at NO_2^- concentration levels as low as 30 μM (Figures 4 and 5). The immediate reaction product, $•NO_2$, is a relatively long lived and moderately strong oxidant that might also cause substantive damage to biological tissues, although this role remains to be established. Nonetheless, a remarkable feature of these reactions is that strong oxidants are generated in reactions that do not involve metal ion catalysis[49] from precursors that are at best only weakly oxidizing, that is, $•NO$, $•O_2^-$, and CO_2. Other putative schemes for biological oxidative damage, notably Fenton reactions involving H_2O_2, require catalysis by redox-active metal ions, which is problematical because metal ions are effectively sequestered in biological tissues.[72]

Acknowledgment. This research was supported by the National Institute of Allergy and Infectious Diseases under Grant AI15834.

IC970946I

(66) Merenyi, G.; Lind, J. *Chem. Res. Toxicol.* **1997**, *10*, 1216.
(67) Adams, G. E.; Aldrich, J. E.; Bisby, R. H.; Cundall, R. B.; Redpath, J. L.; Willson, R. L. *Radiat. Res.* **1972**, *49*, 278.
(68) Chen, S.-N.; Hoffman, M. Z. *Radiat. Res.***1973**, *56*, 40.
(69) Wolcott, R. G.; Franks, B. S.; Hannum, D. M.; Hurst, J. K. *J. Biol. Chem.* **1994**, *269*, 9721.
(70) Lymar, S. V.; Hurst, J. K. *Chem. Res. Toxicol.* **1995**, *8*, 845.
(71) van der Vliet, A.; Eiserich, J. P.; Halliwell, B.; Cross, C. E. *J. Biol. Chem.* **1997**, *272*, 7617.
(72) Halliwell, B.; Gutteridge, J. M. *Methods Enzymol.* **1990**, *186*, 1.